

# Root Cortical Senescence Improves Growth under Suboptimal Availability of N, P, and K<sup>1[OPEN]</sup>

Hannah M. Schneider,<sup>a</sup> Johannes A. Postma,<sup>a</sup> Tobias Wojciechowski,<sup>a</sup> Christian Kuppe,<sup>a</sup> and Jonathan P. Lynch<sup>b,2</sup>

<sup>a</sup>Forschungszentrum Jülich, Institut für Bio- und Geowissenschaften Pflanzenwissenschaften, 52428 Juelich, Germany

<sup>b</sup>Department of Plant Science, Pennsylvania State University, University Park, Pennsylvania 16802

ORCID IDs: 0000-0002-5222-6648 (J.A.P.); 0000-0003-3439-2500 (T.W.); 0000-0002-1837-759X (C.K.); 0000-0002-7265-9790 (J.P.L.).

Root cortical senescence (RCS) in Triticeae reduces nutrient uptake, nutrient content, respiration, and radial hydraulic conductance of root tissue. We used the functional-structural model *SimRoot* to evaluate the functional implications of RCS in barley (*Hordeum vulgare*) under suboptimal nitrate, phosphorus, and potassium availability. The utility of RCS was evaluated using sensitivity analyses in contrasting nutrient regimes. At flowering (80 d), RCS increased simulated plant growth by up to 52%, 73%, and 41% in nitrate-, phosphorus-, and potassium-limiting conditions, respectively. Plants with RCS had reduced nutrient requirement of root tissue for optimal plant growth, reduced total cumulative cortical respiration, and increased total carbon reserves. Nutrient reallocation during RCS had a greater effect on simulated plant growth than reduced respiration or nutrient uptake. Under low nutrient availability, RCS had greater benefit in plants with fewer tillers. RCS had greater benefit in phenotypes with fewer lateral roots at low nitrate availability, but the opposite was true in low phosphorus or potassium availability. Additionally, RCS was quantified in field-grown barley in different nitrogen regimes. Field and virtual soil coring simulation results demonstrated that living cortical volume per root length (an indicator of RCS) decreased with depth in younger plants, while roots of older plants had very little living cortical volume per root length. RCS may be an adaptive trait for nutrient acquisition by reallocating nutrients from senescing tissue and secondarily by reducing root respiration. These simulated results suggest that RCS merits investigation as a breeding target for enhanced soil resource acquisition and edaphic stress tolerance.

Root cortical senescence (RCS) is a type of programmed cell death in Triticeae (Henry and Deacon, 1981; Deacon and Mitchell, 1985). It begins in the epidermis and progresses to inner cortical cell files. However, the literature has suggested that the cortex of axial roots directly adjacent to lateral roots and lateral roots themselves do not undergo senescence. RCS progresses basipetally (Henry and Deacon, 1981) and is anatomically distinct from the formation of root cortical aerenchyma (Deacon et al., 1986; Schneider et al., 2017) and the loss of the root cortex due to secondary growth in dicots (Bingham, 2007).

Previous literature suggests that three main components of RCS may have functional implications: reduced root respiration, reduced radial transport of nutrients and water, and nutrient reallocation from senescing tissues (Robinson, 1990; Schneider et al., 2017). A simple modeling exercise suggests that reallocation of phosphorus

during RCS may be beneficial by supporting new growth (Robinson, 1990). We propose that the remobilization of nitrogen and potassium also may be beneficial when these resources are limiting. Empirical studies have demonstrated that RCS formation reduces the nutrient content of root tissue on a length and dry weight basis, since air spaces in the cortex do not contain nutrients and the stele and cortex have different tissue and nutrient densities (Schneider et al., 2017). Although the amount of nutrients released by senescing cells during RCS is small, over time they may have a significant effect, as an improved plant nutrient status supports greater growth rates and, thus, greater soil exploration in an autocatalytic manner (Wissuwa, 2003; Lynch et al., 2014; Saengwilai et al., 2014).

The metabolic costs of root tissue, including respiration and the investment of scarce resources, including nutrients, are important drivers of plant tolerance to edaphic stress (Zhu et al., 2010; Postma and Lynch, 2011a; Jaramillo et al., 2013; Saengwilai et al., 2014; Chimungu et al., 2015). Respiration is a result of physiological activities such as tissue maintenance, growth, and nutrient uptake. Besides respiration, the metabolic cost of soil exploration also includes root exudates and the investment of nitrogen and phosphorus into tissues. When the soil availability of these nutrients is low, plant growth is reduced and reallocation of these nutrients to

<sup>1</sup> This project was institutionally funded by the Hemholtz Association.

<sup>2</sup> Address correspondence to [jpl4@psu.edu](mailto:jpl4@psu.edu).

The author responsible for distribution of materials integral to the findings presented in this article in accordance with the policy described in the Instructions for Authors ([www.plantphysiol.org](http://www.plantphysiol.org)) is: Jonathan P. Lynch ([jpl4@psu.edu](mailto:jpl4@psu.edu)).

<sup>[OPEN]</sup> Articles can be viewed without a subscription.

[www.plantphysiol.org/cgi/doi/10.1104/pp.17.00648](http://www.plantphysiol.org/cgi/doi/10.1104/pp.17.00648)

growing tissue becomes an important strategy for maintaining new growth, which can increase overall resource capture (Lambers et al., 1996; Lynch and Ho, 2005; Postma and Lynch, 2011a; Lynch, 2015). More than 50% of photosynthate may be allocated to root respiration (Lambers et al., 1996), and the maintenance of cortical tissues account for the majority of the root respiration (Schneider et al., 2017). Root cortical phenes (phene is to phenotype as gene is to genotype; Lynch, 2011; Pieruschka and Poorter, 2012; York et al., 2013), including root cortical aerenchyma, cortical cell size, and cortical cell file number, can influence soil resource capture by regulating the metabolic costs (i.e. carbon and nutrient investment) of soil exploration (Lynch, 2015). In maize (*Zea mays*), the development of root cortical aerenchyma reduces the living cortical area and is associated with improved plant performance in environments with suboptimal water and nutrient availability (Zhu et al., 2010; Postma and Lynch, 2011a; Jaramillo et al., 2013; Saengwilai et al., 2014; Chimungu et al., 2015). Maize lines with reduced living root cortical area due to fewer cell files or greater cell size had improved soil exploration and water acquisition under drought (Chimungu et al., 2014a, 2014b). Reduced living cortical area is associated with reduced root respiration and cortical burden, leading to reduced investment of carbon and other resources into cortical maintenance, permitting greater resource allocation to other plant functions, including growth, resource capture, and reproduction (Lynch and Ho, 2005; Jaramillo et al., 2013; Lynch, 2015).

As with root cortical aerenchyma formation, increased cortical cell size, and reduced cortical cell number, the development of RCS also reduces living cortical tissue. The development of RCS is accelerated in response to deficiencies of mineral nutrients, including phosphorus and nitrogen (Lascaris and Deacon, 1991; Elliott et al., 1993; Schneider et al., 2017). We hypothesized that accelerated RCS formation is an adaptive response under a variety of edaphic stresses by reducing living cortical volume and, thereby, the metabolic cost of soil exploration (Schneider et al., 2017). We have shown previously that excised barley (*Hordeum vulgare*) root segments with RCS have reduced respiration rates ( $\text{g cm}^{-3}$ ) and nutrient content ( $\text{mol cm}^{-3}$ ) compared with segments without RCS (Schneider et al., 2017). We hypothesize that these reductions in metabolic cost associated with RCS formation improve water and nutrient capture in edaphic stress conditions by supporting greater relative growth rates. Root phenes and phene states that increase the exploration of deep soil domains enhance the acquisition of mobile nutrients, including nitrate and water, in many environments (Lynch and Wojciechowski, 2015). These mobile resources are available in deep soil domains over the growing season due to leaching and soil drying from the surface (Lynch, 2013; Trachsel et al., 2013). In contrast, the availability of immobile resources, including phosphate and potassium, is typically greatest in shallow soil domains (Ho et al., 2005; Zhu et al., 2005; Lynch, 2011, 2013). The reduction in the

metabolic costs as a result of RCS may allow the plant to invest in new root growth, reaching deeper soil horizons to obtain mobile nutrients or invest in increased shoot growth and yield.

The senescence of cortical tissue may not always be beneficial to plant growth. The development of root cortical aerenchyma in maize reduced the radial transport of calcium, phosphate, and sulfur (Hu et al., 2014). RCS formation in barley reduced radial hydraulic conductivity and radial nitrogen and phosphorus transport (Schneider et al., 2017). As RCS progresses in root cortical tissue, the apoplastic radial pathways may have fewer intercellular routes and transport may be reduced through the cell-to-cell pathway by reducing the number and surface area of living cells between the epidermis and the stele. As RCS formation progresses and more cortical cells senesce, the continuity of the cell-to-cell pathway is increasingly disrupted. Additionally, RCS formation and root aging coincide with the increased suberization of the endodermis, which also may contribute to reduced hydraulic conductivity (Zimmermann et al., 2000; Baxter et al., 2009; Schneider et al., 2017). It is important to evaluate the additive effects of the functional implications of RCS to determine its effects on whole-plant growth.

Until recently, little quantitative information has been available on the formation of RCS in different root classes and its spatiotemporal distribution. The formation of RCS is complex and dependent on many factors, including genetic and environmental signals (Liljeroth, 1995; Schneider et al., 2017). In addition, root phenes do not function in isolation. Previous studies have demonstrated that root cortical aerenchyma interacts with nodal root number, increasing plant growth up to 130% greater than the expected additive effects. Basal root growth angle interacts with root hair length and density and increased plant growth up to twice the expected additive effect by determining the placement of root hairs in the soil profile (York et al., 2013; Miguel et al., 2015). Understanding how RCS interacts with other phenes for soil resource capture may be an important consideration for breeders (Miguel et al., 2015).

In silico analysis of the functional significance of root phenotypes is a useful complement to empirical analysis (Dunbabin et al., 2013; York et al., 2016; Zhu et al., 2016). Empirical assessment of the utility of RCS formation may be confounded with other root architectural and anatomical phenes, as the generation of isophenic lines is challenging. Simulation studies enable the evaluation of RCS in truly isophenic lines characterized by identical root and shoot phenotypes with a single contrasting phene state, permitting analysis of the effects attributed directly to that phene state, which is generally infeasible in empirical studies (Postma and Lynch, 2011b). *SimRoot*, a functional-structural plant model, also can simulate contrasting environments while holding the plant phenotype constant, which is challenging in empirical studies (Dathe et al., 2016). *SimRoot* results have been useful guides for subsequent empirical work. For example, root cortical aerenchyma in maize, which has

functional similarities to RCS, was predicted by *SimRoot* to have utility in edaphic stress conditions, which was later confirmed by empirical studies in the field and in controlled environments (Postma and Lynch, 2011b; Saengwilai et al., 2014; Chimungu et al., 2015). *SimRoot* predicted enhanced nitrogen capture and biomass in maize/bean/squash polycultures compared with monocultures (Postma and Lynch, 2012), which was later validated in the field (Zhang et al., 2014). The root length density of shallow-rooted common bean (*Phaseolus vulgaris*) genotypes was predicted in *SimRoot* to decrease with depth, which correlated with increased phosphorus capture in the field (Miguel et al., 2015). Decreased inter-root competition, increased topsoil foraging (Ge et al., 2000), and reduced interplant competition (Rubio et al., 2001) were predicted by *SimRoot* to increase phosphorus acquisition in common bean and was validated in the field (Bonser et al., 1996; Zhang et al., 2014). In addition, *SimRoot* predicted sparse lateral branching to have utility in low nitrogen availability (Postma et al., 2014), which was validated in later field and greenhouse studies (Zhan and Lynch, 2015).

This study aims to quantitatively evaluate the potential utility of RCS in barley for nutrient acquisition in a functional-structural plant simulation model that considers root architecture, carbon allocation, and nutrient acquisition. It has been proposed that reallocation of phosphorus during RCS could be beneficial to plant growth (Robinson, 1990). In addition, we propose that reallocation of nitrogen and potassium, reduced root respiration, and reduced radial nutrient uptake could be important functions of RCS in soils with suboptimal nutrient availability. In this study, we evaluate the utility of RCS for the acquisition of nitrogen, phosphorus, and potassium and present, to our knowledge, the first evidence for the interaction of RCS with plant architectural phenes.

## RESULTS

Root microscopy of solution culture-grown plants at 45 d after germination (DAG) demonstrated that RCS does not form in lateral roots of nodal or seminal roots (Supplemental Fig. S1; Supplemental Table S1). Therefore, all results presented (except where noted) reflect data from the formation of RCS exclusively in axial root tissue.

Growth was simulated in *SimRoot* to 80 DAG (Fig. 1). Under suboptimal nitrogen, phosphorus, and potassium availability, RCS increased plant growth and shoot biomass (Fig. 2). Generally, the relative benefit of RCS for growth increased over time (Supplemental Fig. S2). At 80 DAG, nitrogen-deficient plants with RCS were between 5% and 52% larger, phosphorus-deficient plants with RCS were between 14% and 73% larger, and potassium-deficient plants with RCS were between 10% and 41% larger (g dry weight) than plants without RCS. The utility of RCS depended on the deficient nutrient and the severity of the nutrient deficiency. The effect of RCS on plant biomass increased with decreased availability of

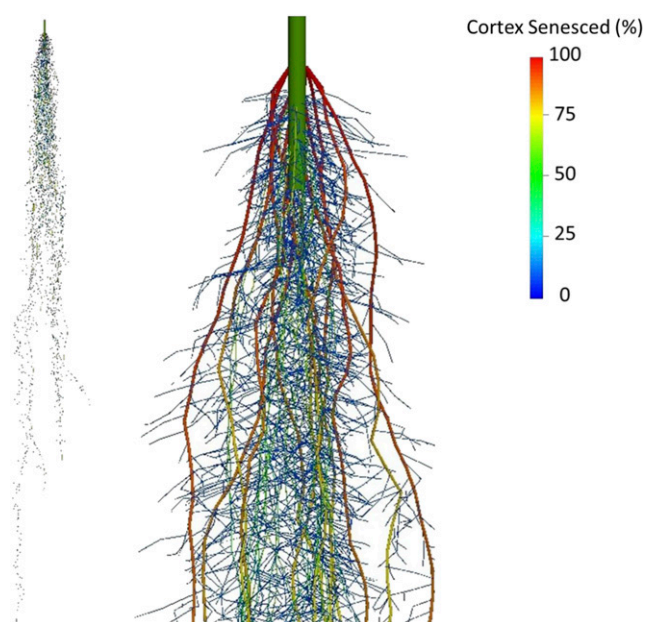


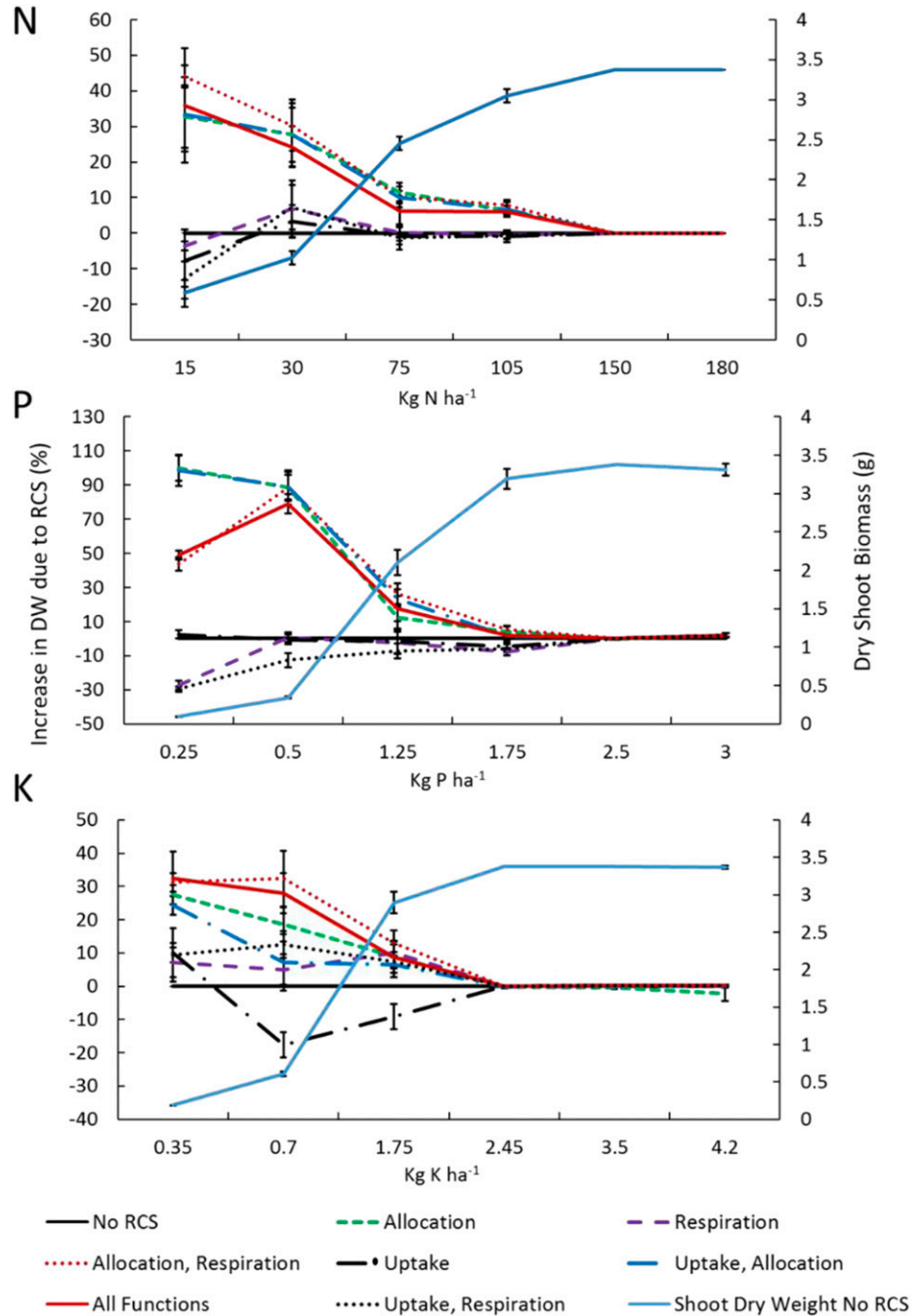
**Figure 1.** Spatial map of RCS formation in simulated barley root systems at 80 DAG. Colors indicate RCS formation as a percentage of the cortical area senesced. Roots have been dilated (approximately 2×) for enhanced visualization and do not indicate true root diameter.

nitrogen and potassium but peaked at moderate levels of phosphorus availability. However, the utility of RCS formation was greatest in phosphorus-replete to moderately deficient conditions (i.e. plant dry weight was 30%–100% of nonstressed plants) and severely deficient conditions (i.e. plant dry weight was 5%–30% of nonstressed plants) compared with potassium or nitrogen. Plants were severely nitrogen deficient at 15 to 30 kg N ha<sup>-1</sup> and moderately deficient at 75 to 150 kg N ha<sup>-1</sup>. Plants were severely phosphorus deficient at 0.25 to 0.5 kg P ha<sup>-1</sup> and moderately deficient at 1.25 to 1.75 kg P ha<sup>-1</sup>. Plants were severely potassium deficient at 0.35 to 0.7 kg P ha<sup>-1</sup> and moderately deficient at 1.75 to 2.45 kg P ha<sup>-1</sup>.

The three proposed RCS functions (root respiration, nutrient uptake, and nutrient reallocation) contributed to the overall benefit of RCS for plant growth under nutrient stress to different degrees. The greatest benefits came from the reallocation of nutrients and, to a lesser extent, reduced root respiration. Reduced nutrient uptake attributed by RCS had a neutral or negative effect on plant growth. Presumably, reallocation of nutrients, respiration, and nutrient uptake occur simultaneously, and the model suggested that these benefits or costs are mostly additive (Fig. 2).

In conditions of suboptimal availability of nitrate, phosphorus, and potassium, reallocation of nutrients from cortical tissue was always beneficial. At 80 DAG, allocation increased plant growth in nitrogen-deficient plants between 10% and 49%, in phosphorus-deficient plants between 9% and 98%, and in potassium-deficient plants between 10% and 37%. The allocation

**Figure 2.** Utility of RCS formation under varying availability of nitrogen, phosphorus, and potassium dissolved in solution at the start of the simulation. Total phosphorus and potassium concentrations are greater due to the buffering capacity (P, 400; and K, 10). On the y axis, the utility of RCS is expressed as a percentage increase in plant dry weight (DW) at 80 DAG. On the secondary y axis, dry shoot biomass is presented for a plant with no RCS. Relative shoot dry biomass was calculated as  $100 \times (X_{RCS} - X_{noRCS})/X_{noRCS}$ . Different lines show the utility for different functions (allocation, respiration, and uptake) of RCS. Error bars represent  $\pm$  SE for four repeated runs. Simulated stochasticity in root growth rates, directions, and branching density causes variation.



of nutrients in the model assumes an equal distribution of nutrients over all organs relative to the nutrient requirements of that organ to function optimally (RNR). We assumed that RCS reduced RNR of the root cortex locally. The development of RCS reduced the total RNR of the whole-root system by up to 26% compared with plants with no RCS. However, under severe phosphorus limitation, RCS increased whole-root system RNR by 4% (Fig. 3; Supplemental Fig. S3). This was due to the increased root growth of these plants and subsequent greater investments of phosphorus compared with phosphorus savings from RCS (Supplemental Figs. S4

and S5). RNR is dependent on the size and age distribution of the root system and RCS. Reallocation of nitrogen during RCS was equivalent to 14% and 5% of the total nitrogen uptake in suboptimal and optimal nitrogen conditions, respectively. At the lowest potassium availability, reallocation of potassium during RCS was equivalent to 10% of the total potassium uptake, and in moderate to optimal potassium conditions, it was equivalent to 3% of the total nutrient uptake. Severe phosphorus deficiency caused changes in root-shoot ratios and subsequently increased root growth. Increased investments of phosphorus in root tissue to

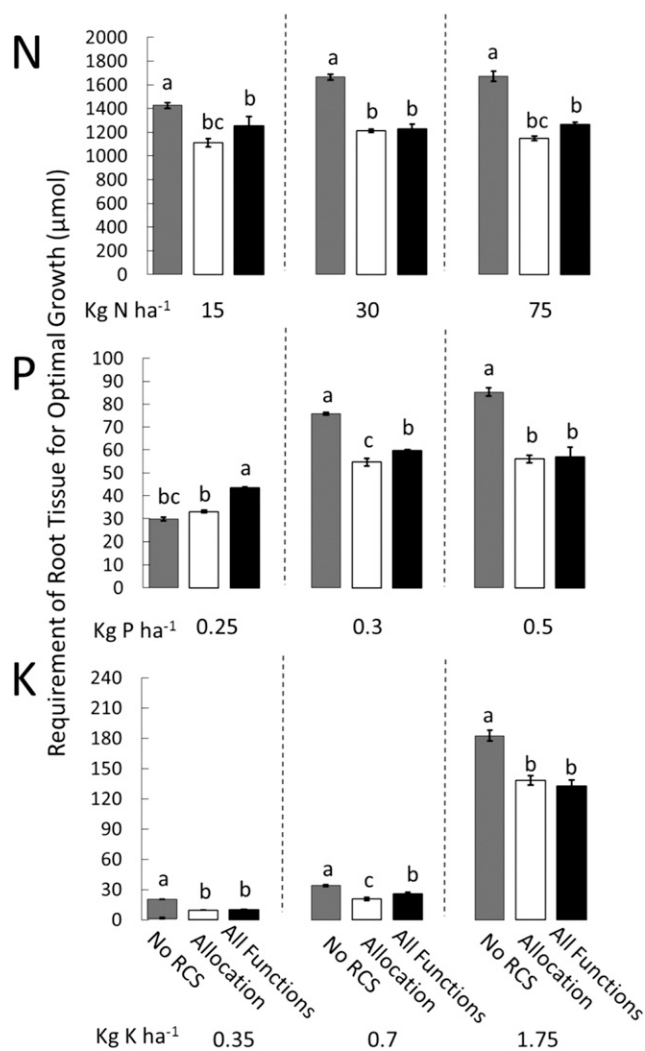


**Figure 3.** RNR ( $\mu\text{mol plant}^{-1}$ ) as affected by RCS and nutrient availability. RCS reduces RNR of the cortex; however, RNR for the whole root system depends on the size and age distribution of the root system. Different bars show the utility for different functions of RCS under suboptimal nitrogen, phosphorus, and potassium availability. Error bars represent SE (see Fig. 2 for explanation). Different letters within the same graph represent significant differences within that graph as determined by Tukey's test ( $P < 0.05$ ). Intermediate and optimal nutrient availability levels showed the same pattern and are depicted in Supplemental Figure S5.

support the increased root length required 40% more phosphorus than the total phosphorus uptake, resulting in severe phosphorus deficiency. At moderate and optimal phosphorus availability, reallocation of phosphorus was equivalent to 16% and 7% of the total nutrient uptake, respectively. Nutrient reallocation from senescing cortical tissues was an important function of RCS and increased plant growth when nutrient availability was limiting.

Reduced root respiration due to RCS was not always beneficial: it decreased plant growth in suboptimal phosphorus availability by 27%, had no effect on growth in low-nitrogen conditions, and increased growth in

suboptimal potassium availability by 7% (Fig. 2). Negative effects of respiration on plant growth are caused by the fact that, in these soils, increased root growth causes a faster increase in RNR than P uptake rates (Supplemental Fig. S5; see "Discussion"). Under low phosphorus availability, a simulated root segment with RCS required 50 d for the nutrient uptake by that segment to be equivalent to the phosphorus invested in that root segment, while root tissue with RCS only required 21.2 d for the phosphorus investment in root tissue to pay off (Supplemental Fig. S5). Simulation of plants with and without RCS enabled evaluation of the reduction in root respiration directly attributed to RCS. Plants with RCS had, on average, 46% less cumulative respiration of the root cortex ( $\text{g C plant}^{-1}$ ) compared with identical plants without RCS, with the largest effects observed under potassium stress (Fig. 4). Reduced root respiration may lead to increased growth if the plant is carbon limited; however, in many scenarios, it increased the nonstructural carbon pool of the whole plant up to 54% at 80 DAG (Fig. 5). Under low nutrient availability, plants with RCS had lower respiration rates per unit root length and lower total respiration rates compared with root systems without RCS, despite the larger root systems of plants with RCS (Supplemental Figs. S4 and S6). Overall, the formation of RCS decreased root respiration and, in most environmental conditions, was beneficial to plant growth.

Another physiological component of RCS, reduced nutrient uptake, had slightly negative or neutral effects on plant growth. Reduced nutrient uptake ( $\mu\text{mol plant}^{-1}$ ) under suboptimal nitrate availability decreased plant growth by 8%. Under moderate potassium stress, reduced nutrient uptake decreased plant growth by 13%. Reduced nutrient uptake under low and moderate phosphorus availability, low potassium availability, and moderate nitrate availability had no effect on plant growth (Fig. 2). At 80 DAG, RCS had relatively small effects on total nutrient uptake of axial, lateral, and fine lateral roots (Supplemental Fig. S7). These negative effects on nutrient uptake were more pronounced during earlier growth stages. At 20 DAG in moderate to optimal nitrogen and phosphorus availability, plants with RCS had 36% and 10% less uptake, respectively, compared with plants with no RCS. RCS had no significant effect on potassium uptake at 20 DAG (Supplemental Fig. S8). In severe nitrogen stress, the axial roots were responsible for the majority of nitrate uptake compared with lateral roots (the axial root develops RCS, and lateral roots do not develop RCS; Fig. 1). In plants with RCS, axial roots had 5% greater total nutrient uptake compared with the total uptake by lateral roots in soils with low nitrogen availability. Plants with no RCS had 23% greater total nutrient uptake by axial roots compared with total root nutrient uptake by lateral roots in conditions of low nitrate availability. In medium to optimal nitrate availability, lateral roots of plants with RCS had 27% greater nutrient uptake compared with nutrient uptake by axial roots. In contrast, plants without RCS had 40%

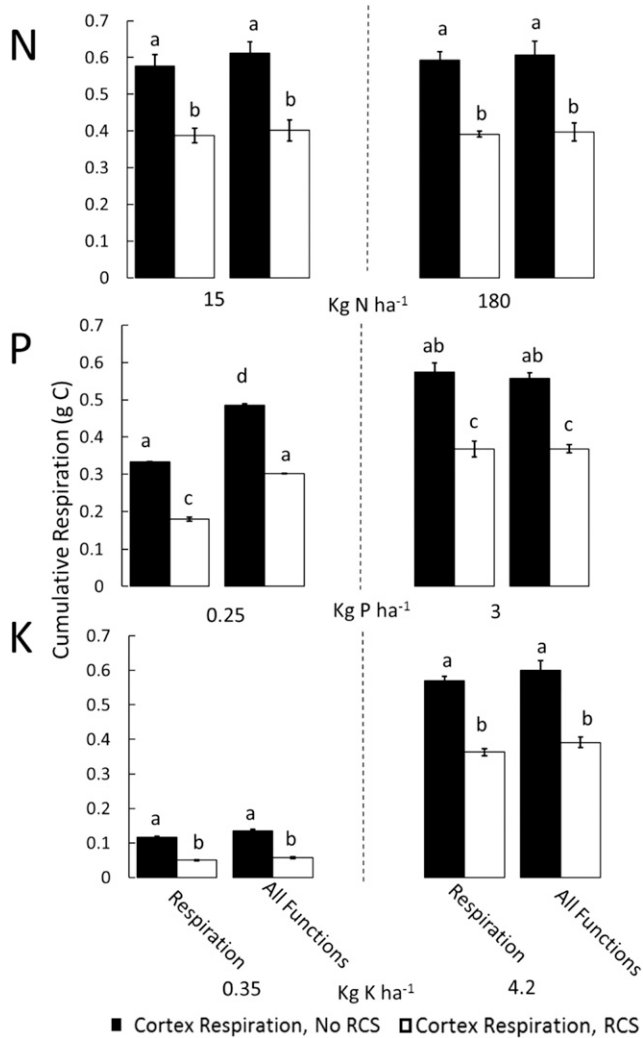


**Figure 4.** Effects of the RCS respiration function on cumulative root respiration in optimal and suboptimal nitrogen, phosphorus, and potassium availability. Cumulative respiration is cortical respiration of the entire root system at 80 DAG. Different bar groups show the utility for different functions of RCS at two levels of nutrient availability (low availability and optimal availability). Cortex Respiration, RCS, Cumulative respiration of the root system cortex after the formation of RCS; Cortex Respiration, no RCS, simulated cumulative respiration of the root system cortex if no RCS has developed. Error bars represent se (see Fig. 2 for explanation). Different letters within the same graph represent significant differences within that graph as determined by Tukey's test ( $P < 0.05$ ).

greater nutrient uptake by axial roots compared with lateral roots. At all levels of phosphorus and potassium availability, the lateral roots accounted for the majority of nutrient uptake compared with axial roots. In environments with a range of phosphorus and potassium availability, lateral roots performed the majority of phosphorus uptake compared with axial roots. Plants with and without RCS had 45% and 39% greater phosphorus uptake, respectively, by lateral roots compared with axial roots. Lateral roots had 27% greater

potassium uptake in plants with RCS and 42% greater potassium uptake in plants with no RCS compared with uptake by axial roots (Fig. 6; Supplemental Fig. S9).

In order to analyze phenotypic synergisms, we simulated the utility of RCS formation under varying nutrient regimes in phenotypes with a varying number of tillers. In optimal nutrient conditions, plants with many tillers and RCS were 9% larger (g dry weight) than plants without RCS and/or with fewer tillers (Fig. 7). In plants lacking RCS, tiller number had no effect on shoot biomass in optimal nutrient conditions due to carbon limitations around 65 DAG. Under nutrient stress, RCS increased plant growth 34% in phenotypes with fewer tillers and 23% in phenotypes with many tillers (Fig. 7). It is important to note that, under suboptimal phosphorus and potassium availability, nutrient deficiencies caused a reduction in the number of tillers formed (three tillers with the potential of forming four tillers). However, contrasts between phenotypes with many tillers (three to four) and few tillers (two) still existed, and the best phenotype in all three low-nutrient soils was one with few tillers and RCS formation. Under severely and moderately suboptimal nitrogen availability, plants with RCS and few tillers had 15% greater biomass compared with the expected additive effects. The synergistic interaction of RCS and few tillers was 23% greater than the expected additive effects under low phosphorus availability and 32% greater than the expected additive effects under low potassium availability. In low and moderate nitrogen, phosphorus, and potassium availability, plants with few tillers and no RCS had between 5% and 27% greater shoot dry weight compared with plants with no RCS and many tillers. Plants with RCS and few tillers had between 10% and 31% greater shoot dry weight in low and moderate nutrient availabilities compared with plants with many tillers.

RCS formation had greater utility in phenotypes with dense lateral branching under low phosphorus and potassium availability, increasing growth by 53% under phosphorus stress and by 29% under potassium stress. In low-nitrogen environments, plants with RCS and sparse lateral branching had 12% greater growth compared with plants with RCS and dense lateral branching (Fig. 8). At the lowest level of nitrogen availability, plants with sparse lateral branching and RCS had 14% greater shoot biomass compared with the expected additive effects. At moderate nitrogen availability, plants with sparse lateral branching and RCS had 21% greater plant biomass compared with the expected additive effects. Under low phosphorus, the synergistic interaction of RCS and dense lateral branching was between 10% and 17% greater than the expected additive effects. Under low potassium, plants with increased lateral branching and RCS had 5% greater shoot biomass compared with the expected additive effects. In moderate phosphorus and potassium conditions, there was a 20% decrease in plant biomass in plants with increased lateral branching and RCS compared with the expected additive effects, which constitutes a functional antagonism.

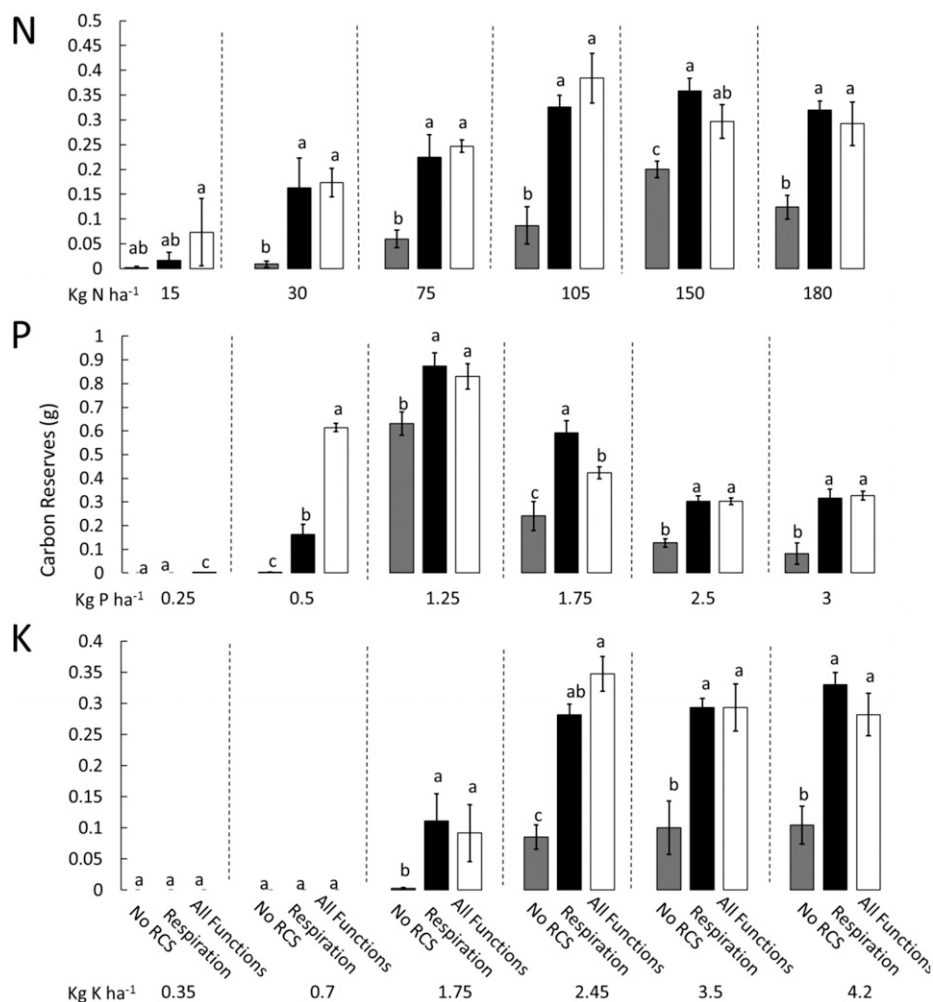


**Figure 5.** Effects of the RCS respiration function on plant carbon reserves. Different bars show the utility for different functions of RCS under varying nitrogen, phosphorus, and potassium availability. The total amount of carbon reserves in the shoot at 80 DAG is represented on the x axis. Error bars represent  $SE$  (see Fig. 2 for explanation). Different letters within the same graph represent significant differences within that graph as determined by Tukey's test ( $P < 0.05$ ).

Simulations were performed evaluating the potential utility of RCS formation in lateral and axial root tissue. The results demonstrated that the formation of RCS in lateral and axial roots was mostly detrimental to plant performance. RCS formation in lateral and axial roots decreased plant growth in suboptimal potassium availability between 9% and 11%, increased plant growth in suboptimal nitrogen availability between 1% and 5%, and decreased plant growth between 1% and 4% in suboptimal phosphorus availability compared with plants with no RCS. However, in optimal nutrient availability, the utility of RCS development in lateral and axial roots was reduced significantly, and plants had between a 22% and 26% decrease in plant growth in optimal nitrogen availability, between an 11% and 17% decrease in plant growth in optimal phosphorus availability, and between a 16% and 19% decrease in plant growth in optimal potassium availability compared with plants with no RCS. The utility of RCS was decreased significantly in plants forming RCS in both lateral and axial roots compared with plants only forming RCS in axial root tissue in all nutrient regimes (Supplemental Fig. S10). Decreases in plant growth due to RCS formation in lateral roots was due to a

significant reduction in total plant nutrient uptake, particularly in moderate to optimal nutrient availability (Supplemental Fig. S11). However, these simulation results only present the potential utility of RCS in lateral roots, as microscopy results confirmed that RCS does not form in first-order lateral roots of nodal and seminal roots of plants at 45 DAG (Supplemental Fig. S1; Supplemental Table S1).

We determined living cortical volume per root length (a proxy for RCS) at different depths in both virtual cores and real cores taken in the field experiment in order to validate the simulated development of RCS in barley root systems. We observed a positive correlation between field and simulation results ( $R^2 = 0.44$ ,  $P < 0.005$ ) at 35 and 80 DAG. At anthesis, the low-nitrogen treatment reduced shoot dry weight by 23% and 27% in simulations and the field, respectively. We separate our data into roots with thin steles (diameter  $> 100 \mu\text{m}$  and  $< 200 \mu\text{m}$ ) and thick steles (diameter  $> 300 \mu\text{m}$ ), as living cortical volume per root length had much more variation with depth in roots with thick steles than with thin steles (Fig. 9). This was presumably due to the continuous production of nodal (i.e. thick-steled) roots throughout plant growth. Lateral roots also are produced

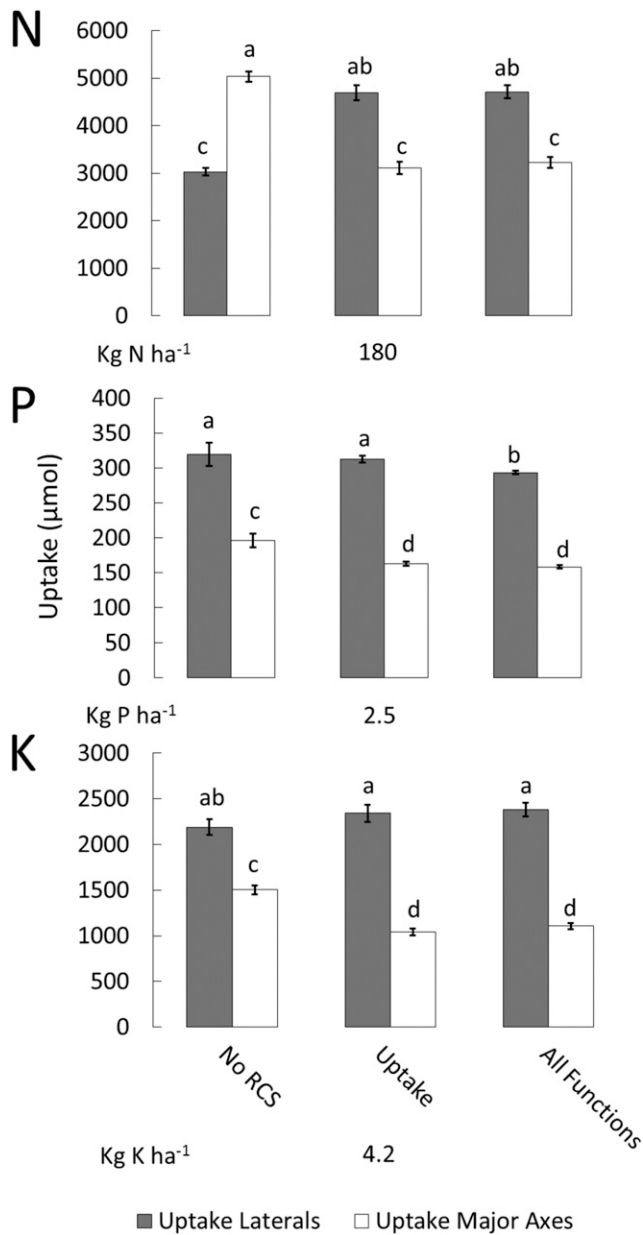


**Figure 6.** Effects of RCS on nitrogen, phosphorus, and potassium uptake in fertile soil. Uptake is the total nutrient uptake at 80 DAG by axial or lateral roots. Different bars show the utility for different functions of RCS. Error bars represent *se* (see Fig. 2 for explanation). Different letters within the same graph represent significant differences within that graph as determined by Tukey's test ( $P < 0.05$ ). Uptake data for suboptimal nutrient availability are depicted in Supplemental Figure S6.

continuously throughout plant growth but do not develop RCS and were not captured in the designated thick and thin stele classes. In roots with a thin stele, living cortical volume per root length increased at depth in younger plants. At anthesis (80 DAG), roots with thin steles had minimal root cortical volume per root length at all depths. Plants grown under low nitrogen had significantly less living cortical volume per root length at depth than plants grown in N-replete conditions. In both

simulations and the field, the amount of living cortical area was minimal in roots with a thick stele, and no significant differences were observed between treatments and small differences were observed between time points (Fig. 9).

**DISCUSSION**

The functional-structural plant model *SimRoot* was used to evaluate the physiological utility of RCS formation in barley under varying nitrogen, phosphorus,

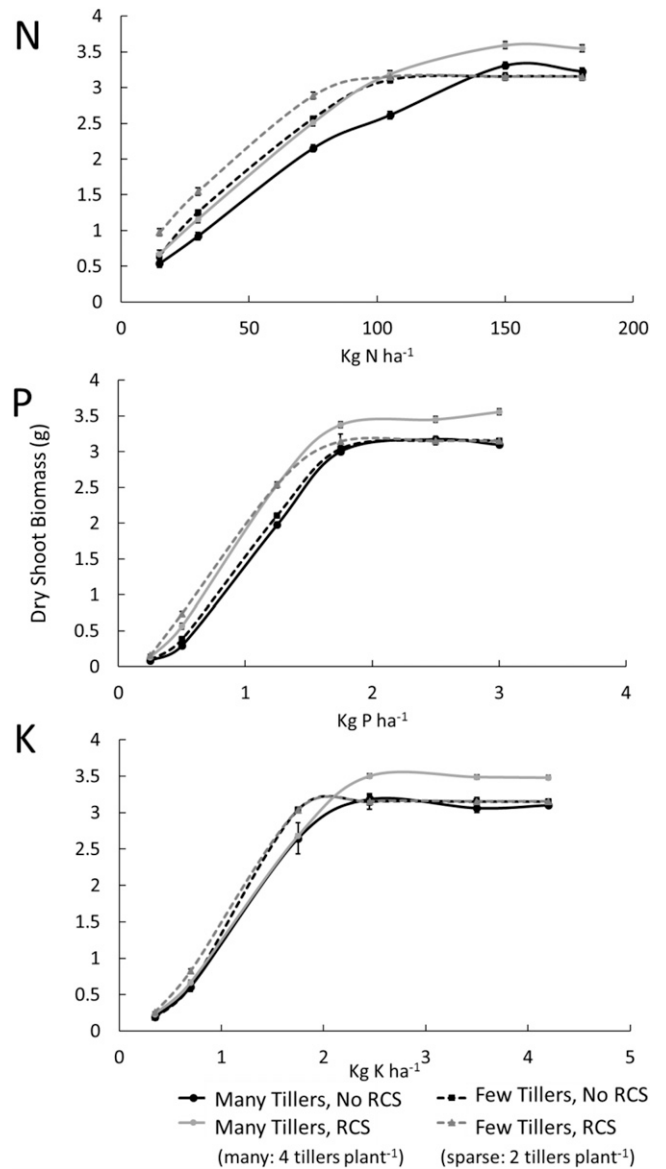


**Figure 7.** Interaction of RCS and tiller number under different availabilities of nitrogen, phosphorus, and potassium. Error bars represent *se* (see Fig. 2 for explanation). Dry shoot biomass is the total dry shoot biomass at 80 DAG. Note that in suboptimal phosphorus and potassium availability, plants with many tillers formed three tillers (with the potential to form four tillers) due to stress conditions.



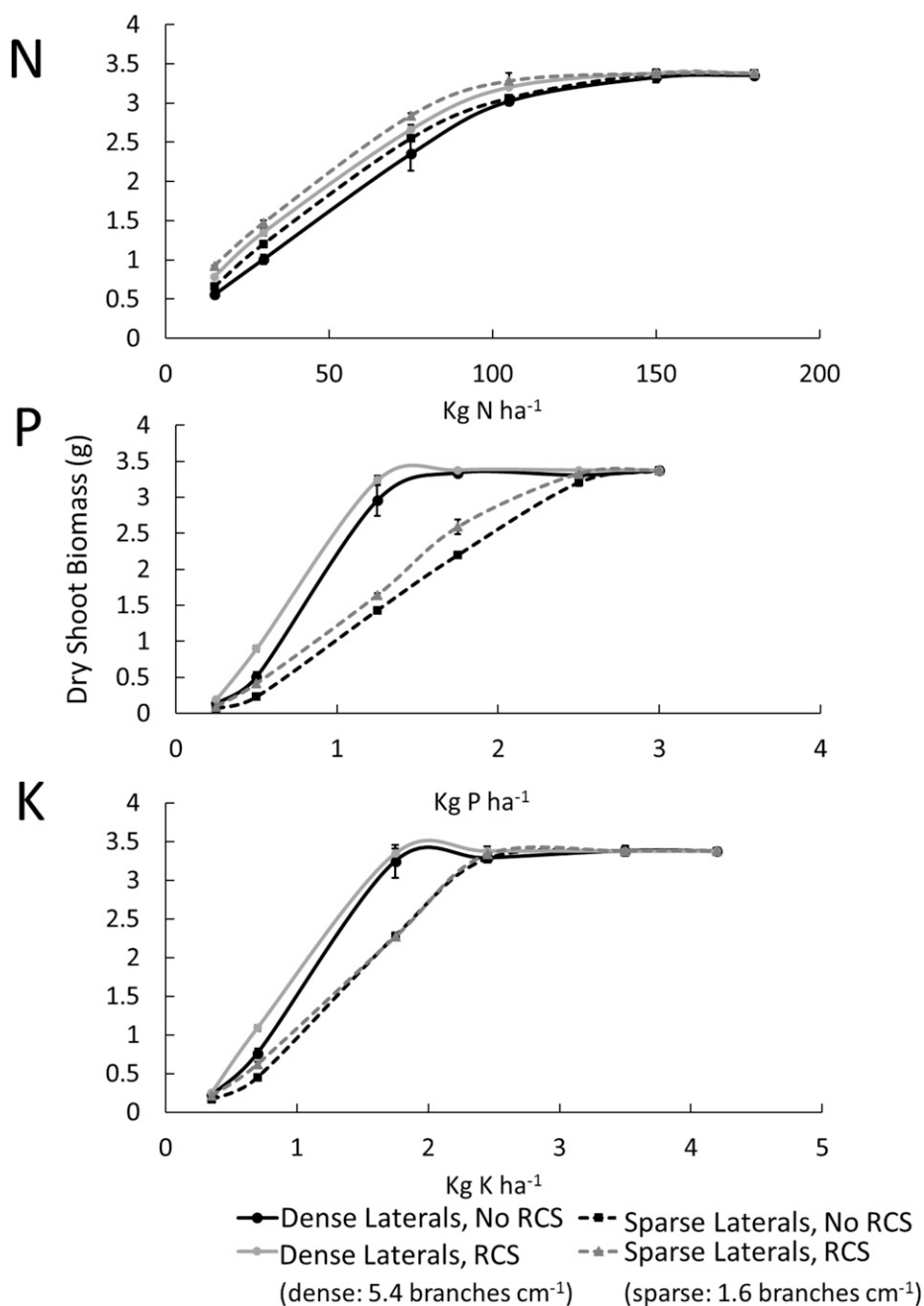


**Figure 8.** Interaction of RCS and lateral branching densities under varying availability of nitrogen, phosphorus, and potassium. Error bars represent SE (see Fig. 2 for explanation). Dry shoot biomass is the total dry shoot biomass at 80 DAG.

and potassium availability. Our results support the hypothesis that RCS is not a symptom of stress injury but may be a useful adaptation under edaphic stress, including suboptimal nutrient availability. Plants with RCS formation had greater plant growth in edaphic stress conditions compared with plants with no RCS formation. The greatest utility of RCS formation was under nutrient stress. Nutrient reallocation, reduced respiration, and reduced nutrient uptake affected the utility of RCS to different degrees (Fig. 2). Plants with RCS had reduced nutrient requirement of root tissue for optimal plant growth ( $\mu\text{mol plant}^{-1}$ ; Fig. 3;

Supplemental Fig. S3), reduced cumulative cortical respiration ( $\text{g C plant}^{-1}$ ; Fig. 4), and increased plant carbon reserves ( $\text{g C plant}^{-1}$ ; Fig. 5). RCS had relatively large effects on total plant nutrient uptake early in growth and smaller effects in later growth stages (Supplemental Figs. S7 and S8). After RCS formation, lateral roots performed the majority of nutrient uptake compared with axial roots (Fig. 6; Supplemental Fig. S9). RCS interacts with other architectural phenes, including lateral branching density and tiller number (Figs. 7 and 8). Living cortical volume, an indicator of RCS, positively correlated in field and simulation results (Fig. 9).

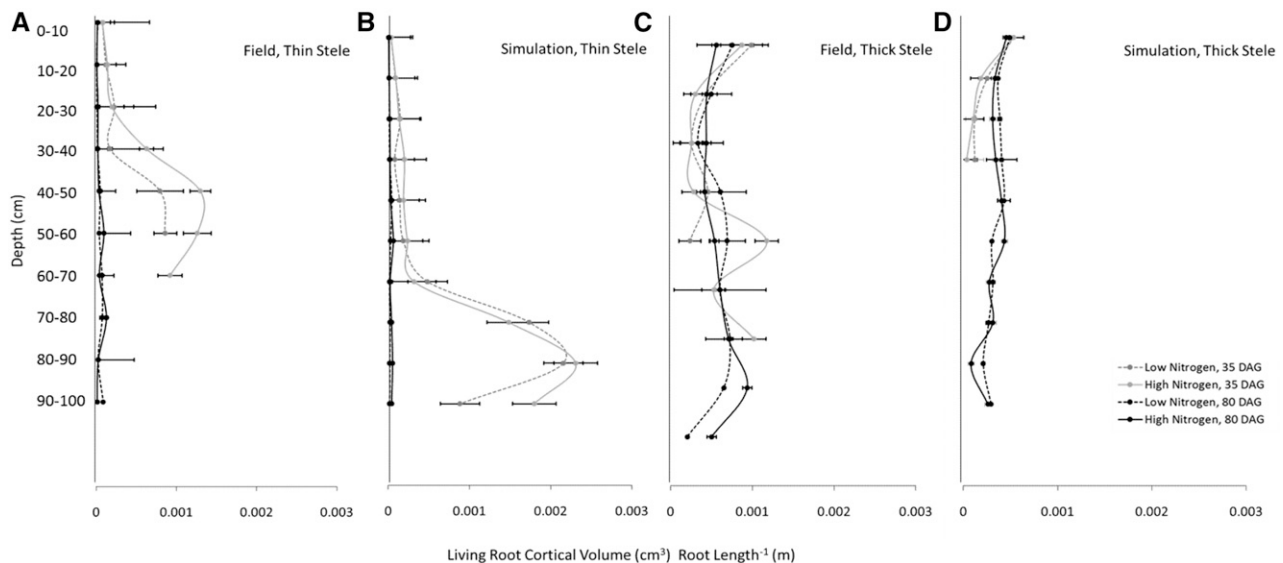


**Figure 9.** Comparison of RCS progression in simulation (A and B) and field (C and D) studies for roots with a thick or thin stele. For field studies, points represent averages of two cores per plot in two replications for four genotypes per treatment. For simulation studies, points represent averages of four replications per treatment. Error bars represent SE.

*SimRoot* predicted nutrient reallocation during RCS to be more important than reduced respiration or nutrient uptake in improving plant growth in suboptimal nutrient availability (Fig. 2). Plants with RCS had a reduced nutrient requirement of root tissue for optimal growth (Fig. 3; Supplemental Fig. S3). These results agree with those of Robinson (1990), who demonstrated that, during RCS, reallocation of phosphorus could be an important function under suboptimal phosphorus availability (Veneklaas et al., 2012; Julia et al., 2016). Our results also demonstrate that reallocation of nitrogen and potassium during RCS formation may improve plant growth, and under suboptimal nutrient availability, nutrient reallocation was equivalent to 10% or greater of the total plant nutrient uptake. The formation of RCS releases a significant amount of nutrients from senescing cells, and over an entire growth season, they may have a significant effect on plant growth, supporting greater growth rates and subsequently greater soil exploration (Lynch et al., 2014; Saengwilai et al., 2014).

Reduced root respiration had relatively small effects on plant growth; however, it had large effects on carbon reserves of the plant (Figs. 2 and 5), which has implications for plant yield (Daniels et al., 1982; Schnyder, 1993; Blum, 1998). Reduced root respiration due to RCS was more important in potassium-deficient plants compared with nitrogen- or phosphorus-deficient plants (Fig. 2). In potassium-deficient plants, root growth is strongly carbon limited compared with plants with nitrogen or phosphorus deficiency. This may be due to a reduction in photosynthesis caused by the deficiency and the lack of an adaptive response in carbon allocation between roots and shoots (Postma and Lynch, 2011b). In nitrogen- or phosphorus-limited conditions, which also may cause a reduction in photosynthesis, carbon allocation to roots

rather than shoots is increased. This results in root growth being less carbon limited in suboptimal phosphorus and nitrogen availability compared with suboptimal potassium availability. In suboptimal nitrogen and phosphorus conditions, reduced respiration results in increased carbon availability and, thus, more root growth (Supplemental Fig. S4). When plant growth is not carbon limited, reductions in respiration rate will simply result in greater accumulation of nonstructural carbon reserves. However, when carbon is limiting root growth, reduced respiration will increase root growth, which may compete with shoot growth for phosphorus resources. In low-phosphorus conditions, the fast relative root growth rate will increase the demand for phosphorus and, thus, increase RNR faster than phosphorus is acquired. New root growth requires the investment of nutrients, and in soils with decreasing nutrient availability, due to leaching and plant uptake, the time it takes for nutrient acquisition to compensate for these investments increases (Supplemental Fig. S5). Therefore, the relative root growth rate should be sufficiently low to be beneficial to the plant in terms of nutrient uptake and continued shoot growth. Fast relative root growth in soils with very low phosphorus availability may not be sustainable. Alternative ways for phosphorus acquisition, which require less phosphorus investment, such as the production of root exudates and the development of mycorrhizal symbioses, may be better strategies in these soils but were not considered in this model.

Root phenes that reduce the metabolic cost of soil exploration by reducing root nutrient content and respiration may enable greater soil exploration (Lynch, 2013). The location of the roots in the soil profile influences the acquisition of specific nutrients. For example, a plant that invests resources into root growth in the

topsoil enhances the acquisition of immobile nutrients such as phosphorus and potassium (Zhu et al., 2005; Lynch, 2013). In contrast, roots located in deeper soil domains enable the capture of mobile nutrients, including water and nitrogen (Lynch, 2013; Trachsel et al., 2013). Root systems may have strategies to capture different nutrients in specific edaphic stress conditions. However, in field environments, multiple stresses may occur simultaneously, which poses a challenge for the optimal location of root growth investments in the soil profile. For example, shallow rooting and topsoil foraging increase phosphorus and other immobile nutrient acquisition; however, they may reduce drought tolerance, as water in drought environments is often located deeper in the soil profile (Ho et al., 2005). The availability of resources in soil domains at which these root investments occur affects the utility of RCS for soil resource capture. Results from this study indicate that RCS may be beneficial for several nutrient deficiencies, including conditions of low nitrogen, phosphorus, and potassium availability. Further studies could investigate the utility of RCS under multiple, simultaneous edaphic stresses.

Changes in nutrient uptake as a result of RCS formation are predicted to have small effects on plant growth. Simulation results showed that lateral roots, which do not develop RCS (Supplemental Table S1; Supplemental Fig. S1), make up 78% of the total root length (data not shown). Root hairs on young root tissue were present in the model; however, in accordance with empirical results, root hairs died off with increasing tissue age and/or the development of RCS (McElgunn and Harrison, 1969). RCS did not have any negative effect on total nutrient uptake of nitrate and potassium compared with plants with no RCS and only small effects on the uptake of phosphorus (Supplemental Fig. S7). Therefore, reduced nutrient uptake by axial roots due to RCS may not have significant effects on total nutrient uptake, as lateral roots perform a large portion of nutrient uptake compared with the axial roots (Fig. 6; Supplemental Fig. S9). In addition, older root segments occupy soil domains that have already been depleted of resources by the younger tissue of the same root axes. Our results show that the reduced nutrient uptake as a result of RCS formation contributes small effects to plant growth in later growth stages and that lateral roots compensate for the reduced uptake of nutrients by axial roots.

Henry and Deacon (1981) observed the formation of RCS in some field-grown lateral roots; however, no systematic study was performed. In this study, we performed a more thorough evaluation of the formation of RCS in lateral roots. Our results demonstrate that RCS does not form in lateral roots (Supplemental Table S1; Supplemental Fig. S1). When RCS formation was simulated in both axial and lateral tissue, plants with RCS had decreased utility compared with plants with no RCS formation in most nutrient regimes (Supplemental Fig. S10). Lateral roots play a large role in plant nutrient uptake, especially after the senescence of axial root cortical tissue (Fig. 6; Supplemental Fig.

S9). We speculate that RCS does not form in lateral root tissue in natural scenarios, as it significantly inhibits plant nutrient uptake, causing detrimental effects to plant growth. We speculate that RCS formation in axial root tissue is an adaptive strategy to maximize nutrient uptake while minimizing the metabolic burden of axial root cortical tissue.

Interaction with other root phenes affected the utility of RCS. RCS had greater utility in plants with fewer tillers (Fig. 7). Each additional tiller added approximately 10 nodal roots (data not shown). In optimal fertility, nutrient uptake was able to support the growth of additional tillers and their nodal roots, which increased soil exploration and, consequently, nutrient acquisition. Under suboptimal fertility, increased tiller number and the development of nodal roots depleted limited soil nutrient resources faster, thereby reducing plant growth as soil nutrient resources became limiting in later growth stages. Lateral branching also affected the utility of RCS (Fig. 8). Greater resource availability as a result of RCS formation allows the plant to grow more root length and, therefore, possibly a greater lateral branching density or length. Dense lateral branching has greater utility for phosphorus and potassium capture compared with nitrogen capture (Postma et al., 2014); thus, a positive interaction exists between increased lateral root branching density and RCS in soils with low phosphorus and potassium availability. However, in nitrate deficiency, decreased lateral branching density has greater utility in plants with RCS due to decreased intraroot and interroot (monoculture) competition (Zhan and Lynch, 2015). We demonstrated that the utility of RCS depends on interactions with other phenes, including the number of tillers and lateral root branching density. We hypothesize that RCS may have synergistic interactions with phenes that are beneficial for soil resource acquisition but that have a high metabolic cost. For example, a root phene with a high metabolic cost, the number of nodal roots, and a phene that reduces the metabolic cost of the root, root cortical aerenchyma, interact in maize (York et al., 2013). Synergisms also may exist with phenes that effect root placement in soil domains. For example, a steep growth angle increases nitrogen capture in some N regimes (Trachsel et al., 2013; Dathe et al., 2016). Phene synergisms show strong interactions with environmental conditions and, therefore, may be important drivers in evolution and should be considered in crop breeding.

The spatiotemporal progression of RCS was similar in field and in silico environments. Living cortical volume per root length is more stable over time and depth in roots with a thin stele, presumably due to the uniform emergence of seminal roots at a specific growth stage, whereas new nodal roots emerge throughout tiller development. Within a soil core, roots with a thick stele may have dramatically different ages due to the continuous development of nodal roots. Phenotyping RCS in the field is challenging, as it is difficult to determine the age, length, and root class of individual roots. The progression of RCS as quantified by living

cortical volume per root length correlates well with RCS development in soil, solution culture, and controlled environments, which were the basis for our model parameterization (Schneider et al., 2017). In the portion of roots with a thin stele in young plants, RCS generally progressed faster in low-nitrogen conditions compared with high-nitrogen conditions (Fig. 9).

The formation of RCS was always beneficial, increasing plant growth under edaphic stress. Genetic variation for the formation of RCS exists (Deacon and Lewis, 1982; Liljeroth, 1995), which may indicate that tradeoffs exist for RCS formation. This *SimRoot* study considered the tradeoff of reduced nutrient uptake. However, other potential tradeoffs of RCS formation are poorly understood. The loss of the cortex may have negative implications for plant fitness, including reduced mycorrhizal symbiosis caused by reduced cortical habitat, altered response to pathogens, and reduction in the ability of sequester toxic ions, including Na and Cl, under salinity stress (Schneider et al., 2017). This study did not consider these tradeoffs, and it is unclear to what extent they may affect the conclusions. However, the constitutive development of RCS in barley, wheat (*Triticum aestivum*), and other crops suggests that the benefits of RCS formation outweigh the potential tradeoffs (Liljeroth, 1995). Model parameterization was limited to 80 DAG. Data for parameterization for root and RCS development of older plants are needed in order to simulate full plant life cycles, which may provide insights into the effects of RCS on grain yield. An integrated and quantitative approach is needed to develop a model to study these interactions.

Here, we present, to our knowledge, the first implementation of *SimRoot* for barley. This is noteworthy since, unlike previous implementations of *SimRoot*, barley is a tillering species, which presents unique root phenotypes, as well as modeling challenges, and is a step toward simulation of other important tillering species such as wheat and rice. In silico analysis of the functional implications of RCS is a valuable complement to empirical analysis. Simulations permit the evaluation of phenotypes and scenarios that are inaccessible to empirical research (e.g. RCS development in lateral roots) and enable the evaluation of isophenic lines, which is generally infeasible in empirical studies. Simulations also enable evaluation of the utility and relative contributions of different functions of RCS (allocation, respiration, and nutrient uptake) independently and in many more nutrient regimes and phenotypic backgrounds than time and resources would allow for empirical studies. The complexity of the soil environment and phenotypic background and the large number of potential interactions and scenarios demand in silico analysis with functional-structural plant models such as *SimRoot*.

## CONCLUSION

*SimRoot* can be used to simulate the utility of RCS in variable environments. Functional-structural plant models are a valuable tool for evaluating the utility of

phenes and breeding strategies that target specific root phenes. Quantitative support from simulation has been provided for the hypothesis that reduced root respiration, reduced nutrient uptake, and reallocation of nutrients caused by RCS formation affect plant growth. The additive interactions of these three functions improve plant growth under nutrient limitation. The reallocation, respiration, and nutrient uptake functions all have positive and negative feedbacks in the model. Simulation permitted us to consider these feedbacks independently as well as simultaneously. Negative feedbacks may be caused by slight disturbances in nutrient homeostasis of the plant. However, in real plants, all functions occur together, and we speculate that negative feedbacks are mitigated and that RCS may have a net positive influence on plant growth. These results indicate that RCS may be an adaptive response for plant growth in environments with low nutrient availability or intense belowground competition, which include most terrestrial ecosystems. The utility of RCS in environments with low nitrogen, phosphorus, and potassium availability depends on interactions between other root phenes and environmental factors. In this study, the utility of RCS was enhanced with different levels of lateral root branching and number of tillers in nutrient-limited conditions. RCS has potential utility for improved plant performance under several edaphic stresses and merits empirical investigation and confirmation. Crops with enhanced soil resource acquisition would be useful in global agriculture, and we propose that these results may be analogous to other species that also form RCS, including wheat, oat (*Avena sativa*), and triticale.

## MATERIALS AND METHODS

*SimRoot*, a functional-structural plant model (Lynch et al., 1997; Postma and Lynch, 2011a, 2011b; Dathe et al., 2016), was used to simulate root growth and plant performance. The model simulates distinct root classes, and root architecture is composed of discrete small (e.g. 1 cm) connected root segments. Root growth and soil resource acquisition are simulated transiently in three-dimensional virtual soil. A soil module, which can simulate water flow and solute transport (Šimunek et al., 1995), is integrated with the root architecture module. A finite element method containing nodal values for water content, nutrient content, and soil properties solves the Richards equation for unsaturated water flow and the convection-dispersion equation for solute transport. The development of depletion zones is caused by water flowing toward the roots during nutrient and water uptake by roots, which may cause interroot competition. Total nutrient uptake of the entire root system is calculated by integrating nutrient uptake over all root segments.

Coupled to the root system is a shoot model, which simulates the development of leaves, tillers, and stems. Growth of the shoot is regulated such that nutrient homeostasis is achieved. A light-capture and photosynthesis model provides the plant with carbon. Tillers form their own leaf area and their own nodal root system. Discrepancies between the source and sink strength of the plant are balanced by carbon reserves coming from the seed and a nonstructural carbon pool. When these carbon reserves do not suffice, growth is reduced.

## Model Description

*SimRoot* was described previously (Lynch et al., 1997; Postma and Lynch, 2011a, 2011b). We extended *SimRoot* by including a new root water uptake and RCS module. *SimRoot* is now open source (*OpenSimRoot*) and fully programmed in C++, which improves code efficiency, reusability, and the modular structure of *SimRoot*. We simulated plant growth with the formation of RCS with three different functions, nutrient uptake, allocation, and respiration, and combinations of

these functions in a multifactor analysis. RCS was represented in the model as a time- and root class-dependent volumetric percentage that affects root respiration, nutrient allocation, and/or nutrient uptake. RCS develops in seminal and nodal roots and progresses over time, decreasing root respiration and nutrient uptake and potentially affecting nutrient allocation as cortical cells senesce (Schneider et al., 2017). The parameterization of RCS formation and its effects was based on measurements of individual roots (Schneider et al., 2017), and RCS only developed in axial root tissue of seminal and nodal roots (unless where noted). RCS reduced the respiration and nutrient content of the cortex proportionally. We split up the root diameter into the diameter of the stele and the cortex. Reduction in nutrient content of the cortex was assumed not to reduce the total amount of nutrients in the plant. Consequently, only the amount of nutrients needed for optimal plant growth was reduced and, thereby, the ratio between nutrient demand and actual nutrient uptake, which is defined as a plant growth stress factor. Therefore, RCS directly alleviates stress and reduces carbon consumption, allowing for greater carbon investment in structural growth. As a cost, however, we simulated that RCS reduces both the hydraulic conductivity and the root kinetics for nutrient uptake. We assumed that the maximum uptake rate ( $I_{max}$ ) was reduced but that the sensitivity (here defined as  $I_{max}/K_m$ ) was not by equally reducing both parameters of the Michaelis-Menten kinetics equation.

We implemented the architectural root water uptake model for a growing root system with a (current) network analogy (time and space dependency). A network analogy to address segment-based root water uptake (i.e. root architecture) was presented by Doussan et al. (1998) and based on the equations of Alm et al. (1992) that describe the similarity to a finite element representation (for a linear root system). In this model, the root system is represented by a number of segments that have an axial and radial hydraulic conductivity associated with them. Boundary conditions include a collar potential and, for each root segment, an outside water potential. We adapted the model to work with a growing root system and used a Newton solver to iteratively determine the collar potential such that the water uptake of the root system equals the potential transpiration, as estimated by the Penman-Monteith equation (Monteith, 1965; for details, see Postma et al., 2017). The outside water potential was obtained by coupling the root model to the soil model as described by Postma and Lynch (2011a). Thus, the root water uptake model in the end only determined the distribution of water uptake over the root system, not the total water uptake. In our scenarios, the soil was sufficiently wet such that drought (in the form of very low collar potentials) did not occur.

Axial and radial hydraulic conductivity were given as root class- and age-dependent inputs and were scaled according to root segment length and surface area, respectively, where greater length reduced the axial conductivity whereas greater surface area increased the radial conductivity proportionally. When RCS (age) reduced the hydraulic conductivity of older root segments, additional water was being taken up by younger root segments. Water uptake affected the convective flow of nitrate toward the roots, such that the reduced hydraulic conductivity of older roots might cause greater mass flow toward younger roots. Thus, reduced hydraulic conductivity might actually function as a benefit and not a tradeoff of RCS.

## Simulated Scenarios and Environments

Environmental conditions were varied to include six levels of nitrogen, phosphorus, and potassium nutrient availability. Barley (*Hordeum vulgare*) growth was simulated over 80 DAG. A single barley plant was simulated not in isolation but as a representative individual in a monoculture field. Plant density was 333 plants  $m^{-2}$ . Depth of the soil profile was 200 cm, row spacing was 10 cm, and distance within the row was 3 cm. At the start of the simulation, a seed was germinated in the middle of a 10- × 3- × 200-cm column. Accurate root density was achieved by mirroring the roots at the boundary back into the column (Postma and Lynch, 2011b).

Simulations were performed in a full-factorial design. Four different experiments were performed: (1) varying nitrate, phosphorus, or potassium availability and all possible combinations of the three different functions of RCS (allocation, uptake, and respiration) formation in axial roots; (2) varying nitrate, phosphorus, or potassium availability with all combinations of the three different functions of RCS in axial roots with two different levels of lateral branching density; (3) varying nitrate, phosphorus, or potassium availability with all combinations of the three different functions of RCS in axial roots with two different levels of tiller number; and (4) varying nitrate, phosphorus, or potassium availability and all possible combinations of the three different functions of RCS (allocation, uptake, and respiration) formation in axial and lateral roots. Initial nutrient availability in the soil was varied at six levels (nitrate, 15, 30, 75, 105, 150, and 180  $kg\ ha^{-1}$ ; phosphate, 0.25, 0.5, 1.25, 1.75, 2.5,

and 3  $kg\ ha^{-1}$ ; potassium, 0.35, 0.7, 1.75, 2.45, 3.5, and 4.2  $kg\ ha^{-1}$ ). In all treatments, the initial relative distribution of nutrients in the soil was kept the same. The nitrate mineralization rate also was scaled relative to the total initial amount of nitrate in the columns. These nitrate, phosphorus, and potassium levels were chosen as they represent a range of stress levels ranging from severe stress resulting in severely reduced (~95%) shoot growth to no stress. Lateral root branching densities were set at two levels for the synergism study (high, 5.4 branches  $cm^{-1}$ ; and low, 1.6 branches  $cm^{-1}$ ) based on lateral branching density data in barley (Drew, 1975, H.M. Schneider, unpublished data). Tiller number was set at two levels for the synergism study (high, 4; and low, 2) based on tiller number data in barley (Hecht et al., 2016).

Root growth rate parameters were taken from phenotyping measurements performed in the greenhouse at the Forschungszentrum Jülich and in the field (Hecht et al., 2016; V. Hecht, unpublished data). Growth rates decreased over time, and different root classes and developmental stages were taken into account. The seminal roots emerged from the seed. Nodal roots emerged later from the stem. All roots had the potential to develop laterals of first and second order.

A fine-textured loam was simulated based on a field environment in Bonn, Germany, that commonly supports barley growth. Soil parameters are described in Supplemental Appendix S2. Climate and precipitation data for 80 d beginning on March 25 were taken from a field weather station in Klein Altendorf, Germany, and was averaged over four years (2012 × 2015). Input files with all parameter values are given in Supplemental Appendix S2.

In order to compare simulation results with field data (see below), soil cores 100 cm in length and 2 cm in diameter were simulated. The core was taken directly over each plant in four replications for two treatments (high nitrogen [180  $kg\ ha^{-1}$ ] and low nitrogen [75  $kg\ ha^{-1}$ ]). Nitrogen levels were selected based on a comparable biomass reduction to the field (below) due to low nitrogen availability. Each core was divided vertically into 10-cm segments. Roots were divided into two classes based on stele diameter (thick, diameter > 300  $\mu m$ ; or thin, diameter > 100  $\mu m$  and < 200  $\mu m$ ). The length and volume of living cortical area were measured for each root.

## Statistical Analysis

A total of 3,792 simulations were run. All computations were run on the cluster plabipd hosted at the Forschungszentrum Jülich. To reduce noise introduced by the random number generator, four repetitions were necessary, and variation among replications is due to stochasticity in growth rates and branching frequency within the same root class. Data were analyzed by paired Student's *t* tests, Pearson correlation coefficients, and Tukey's honestly significant difference test in R 3.1.2 (R Core Team, 2014). Significant differences only indicate that results are unlikely to be artifacts of the random number generator.

## Field Studies

Four barley genotypes (Nuereburg, Golf, Arena, and Tkn24b) were used in field studies. Genotypes Nuereburg and Tkn24b are landraces, and Golf and Arena are modern varieties. Tkn24b is from Nepal, Nuereburg and Arena are from Germany, and Golf is from the United Kingdom. Landraces typically have a faster progression of RCS compared with modern varieties (Schneider et al., 2017). Genotypes were selected for contrasting RCS based on previous screening studies (data not shown).

Genotypes were planted in two replications under both high and low nitrogen availability in a loamy silt soil at Campus Klein Altendorf (50°36'47''N, 6°59'39.3''E) on March 23, 2016. Due to equipment errors, the Nuereburg genotype was only planted in one replication. Planting density was 87 plants  $m^{-2}$  in plots 0.95 m in length and 1.5 m wide. On April 27 and June 16, 2016, soil cores 2 cm in diameter were taken directly over two randomly selected plants in each plot to a depth of 100 cm. These dates were chosen because 35 DAG is when RCS has developed in both seminal and nodal roots (Schneider et al., 2017) and 85 DAG is anthesis. The core was divided into 10-cm segments. Cores were washed carefully to extract the roots, and roots were preserved in 75% ethanol. For each root, the length was measured by scanning and analyzing preserved root segments using WinRHIZO Pro (Régent 389 Instruments). After length analysis, each root was stained with Acridine Orange for anatomical analysis.

## Solution Culture Studies

Seeds of two barley genotypes (Nuereburg and Golf) were surface sterilized in 1.5% (v/v) NaOCl in water and then transferred to germination paper (76 lb; Anchor Paper). Seeds were rolled in the germination paper into tubes and placed in

covered beakers containing 0.5 mM CaSO<sub>4</sub>. Beakers were placed in a dark climate chamber at 28°C for 4 d. Next, the beaker was placed under a fluorescent light (350 μE m<sup>-2</sup> s<sup>-1</sup>) for 1 d. Five germinated seedlings were transferred to each 33-L solution culture tank. Seedlings were randomly assigned foam plugs suspended above each tank. Plants were grown in solution culture in a climate chamber (22°C, 12 h of daylight, and 50% relative humidity) for 30 d. The nutrient solution (pH 5.5) contained 2.5 mM KNO<sub>3</sub>, 2.5 mM Ca(NO<sub>3</sub>)<sub>2</sub>, 1 mM MgSO<sub>4</sub>, 0.5 mM KH<sub>2</sub>PO<sub>4</sub>, 50 μM NaFeEDTA, 0.2 μM Na<sub>2</sub>MoO<sub>4</sub>, 10 μM H<sub>3</sub>BO<sub>3</sub>, 0.2 μM NiSO<sub>4</sub>, 1 μM ZnSO<sub>4</sub>, 2 μM MnCl<sub>2</sub>, 0.5 μM CuSO<sub>4</sub>, and 0.2 μM CoCl<sub>2</sub>. The pH of the nutrient solution was adjusted to 5.5 daily using KOH, and the complete solution was replaced weekly.

After 45 DAG, plants were harvested from solution culture. In three replications, lateral roots were sampled for each genotype at three positions (8–10 cm, 18–20 cm, and 28–30 cm from the root apex) on seminal and nodal axial roots. Sampled lateral root segments were preserved in 70% ethanol for Acridine Orange staining.

## Anatomical Analysis

Acridine Orange staining was performed according to Henry and Deacon (1981), except that the staining time was extended to 30 min. After staining, roots were embedded in a gelatin capsule using Tissue-Tek CRYO-OCT compound (Fisher Scientific). Transverse cross sections 60 μm thick were cut using a Kryostat 2800 Frigocut-E (Reichert-Jung, Leica Instruments). Images of cross sections were acquired on a compound microscope (Axioplan 2, mounted with an AxioCam ICc 5, Filter 09: Blue 450–490 nm; Carl Zeiss; 20× magnification). For solution culture experiments, the total number of cortical cell files and the number of cortical cell files with at least one viable nucleus were recorded. Acridine Orange fluorescent nuclei were used to phenotype RCS, and the disappearance of the cortex, as determined by the number of viable cortical cell files, was used to phenotype RCS on a root cross-sectional level.

For field experiments, root cross sections were analyzed for stele diameter and the amount of living cortical area. The length of the root was multiplied by the amount of living cortical area for each section to determine the living cortical volume of each root segment. The root segments were classified by their stele diameter as a thick root (diameter > 300 μm) or a thin root (diameter > 100 μm and < 200 μm). These diameter classes exclude lateral roots and capture the majority of nodal and seminal roots. The total living cortical volume in each 10-cm soil slice was summed and divided by the total root length of the appropriate diameter class in that slice. Data were analyzed using Pearson correlation coefficients in R 3.1.2 (R Core Team, 2014).

## Supplemental Data

The following supplemental materials are available.

**Supplemental Figure S1.** RCS formation in first-order lateral roots of nodal and seminal roots 45 DAG.

**Supplemental Figure S2.** Effects of RCS on plant growth over time under varying availability of nitrogen, phosphorus, and potassium.

**Supplemental Figure S3.** Effects of the RCS allocation function on the requirement of root tissue for optimal plant growth.

**Supplemental Figure S4.** Effects of RCS on total root length under varying availability of nitrogen, phosphorus, and potassium at 80 d of growth.

**Supplemental Figure S5.** Investment of phosphorus and subsequent pay-off in root tissues with and without RCS.

**Supplemental Figure S6.** Effects of RCS on the respiration rate per root length under varying availability of nitrogen, phosphorus, and potassium at 80 d of growth.

**Supplemental Figure S7.** Effects of RCS on total nutrient uptake under varying availability of nitrogen, phosphorus, and potassium at 80 DAG.

**Supplemental Figure S8.** Effects of RCS on total nutrient uptake under varying availability of nitrogen, phosphorus, and potassium at 20 DAG.

**Supplemental Figure S9.** Effects of RCS on nitrogen, phosphorus, and potassium uptake under suboptimal nutrient availability.

**Supplemental Figure S10.** Utility of RCS formation in axial and lateral roots under varying availability of nitrogen, phosphorus, and potassium dissolved in solution at the start of the simulation.

**Supplemental Figure S11.** Effects of RCS in axial and lateral roots on total nutrient uptake under varying availability of nitrogen, phosphorus, and potassium at 80 DAG.

**Supplemental Table S1.** RCS formation in first-order lateral roots of nodal and seminal roots at 45 DAG.

**Supplemental Appendix S1.** Root water uptake model.

**Supplemental Appendix S2.** *SimRoot* parameterization.

## ACKNOWLEDGMENTS

We thank Vera Hecht for parameterizing the barley root model and Tanja Ehrlich and Vera Boeckem for helping with soil coring.

Received May 16, 2017; accepted June 25, 2017; published June 30, 2017.

## LITERATURE CITED

- Alm DM, Cavalier J, Nobel PS (1992) A finite-element model of radial and axial conductivities for individual roots: development and validation for two desert succulents. *Ann Bot (Lond)* **69**: 87–92
- Baxter I, Hosmani PS, Rus A, Lahner B, Borevitz JO, Muthukumar B, Mickelbart MV, Schreiber L, Franke RB, Salt DE (2009) Root suberin forms an extracellular barrier that affects water relations and mineral nutrition in *Arabidopsis*. *PLoS Genet* **5**: e1000492
- Bingham IJ (2007) Quantifying the presence and absence of turgor for the spatial characterization of cortical senescence in roots of *Triticum aestivum* (Poaceae). *Am J Bot* **94**: 2054–2058
- Blum A (1998) Improving wheat grain filling under stress by stem reserve mobilisation. *Euphytica* **100**: 77–83
- Bonser AM, Lynch J, Snapp S (1996) Effect of phosphorus deficiency on growth angle of basal roots in *Phaseolus vulgaris*. *New Phytol* **132**: 281–288
- Chimungu JG, Brown KM, Lynch JP (2014a) Reduced root cortical cell file number improves drought tolerance in maize. *Plant Physiol* **166**: 1943–1955
- Chimungu JG, Brown KM, Lynch JP (2014b) Large root cortical cell size improves drought tolerance in maize. *Plant Physiol* **166**: 2166–2178
- Chimungu JG, Maliro MFA, Nalivata PC, Kanyama-Phiri G, Brown KM, Lynch JP (2015) Utility of root cortical aerenchyma under water limited conditions in tropical maize (*Zea mays* L.). *Crop Res* **171**: 86–98
- Daniels RW, Alcock MB, Scarisbrick DH (1982) A reappraisal of stem reserve contribution to grain yield in spring barley (*Hordeum vulgare* L.). *J Agric Sci* **98**: 347–355
- Dathe A, Postma JA, Postma-Blaauw MB, Lynch JP (2016) Impact of axial root growth angles on nitrogen acquisition in maize depends on environmental conditions. *Ann Bot (Lond)* **118**: 401–414
- Deacon J, Drew M, Darling A (1986) Progressive cortical senescence and formation of lysigenous gas space (aerenchyma) distinguished by nuclear staining in adventitious roots of *Zea mays*. *Ann Bot (Lond)* **58**: 719–727
- Deacon J, Lewis SJ (1982) Natural senescence of the root cortex of spring wheat in relation to susceptibility to common root rot (*Cochliobolus sativus*) and growth of a free-living nitrogen-fixing bacterium. *Plant Soil* **66**: 13–20
- Deacon JW, Mitchell RT (1985) Comparison of rates of natural senescence of the root cortex of wheat (with and without mildew infection), barley, oats and rye. *Plant Soil* **84**: 129–131
- Doussan C, Pages L, Vercambre G (1998) Modelling of the hydraulic architecture of root systems: an integrated approach to water absorption—model description. *Ann Bot (Lond)* **81**: 213–223
- Drew M (1975) Comparison of the effects of a localized supply of phosphate, nitrate, ammonium and potassium on the growth of the seminal root system, and the shoot, in barley. *New Phytol* **75**: 479–490
- Dunbabin VM, Postma JA, Schnepf A, Pagès L, Javaux M, Wu L, Leitner D, Chen YL, Rengel Z, Diggle AJ (2013) Modelling root-soil interactions using three-dimensional models of root growth, architecture and function. *Plant Soil* **372**: 93–124
- Elliott B, Robson A, Abbott L (1993) Effects of phosphate and nitrogen application on death of the root cortex in spring wheat. *New Phytol* **123**: 375–382

- Ge Z, Rubio G, Lynch JP (2000) The importance of root gravitropism for inter-root competition and phosphorus acquisition efficiency: results from a geometric simulation model. *Plant Soil* **218**: 159–171
- Hecht VL, Temperton VM, Nagel KA, Rascher U, Postma JA (2016) Sowing density: a neglected factor fundamentally affecting root distribution and biomass allocation of field grown spring barley (*Hordeum vulgare* L.). *Front Plant Sci* **7**: 944
- Henry C, Deacon J (1981) Natural (non-pathogenic) death of the cortex of wheat and barley seminal roots, as evidenced by nuclear staining with acridine orange. *Plant Soil* **60**: 255–274
- Ho MD, Rosas JC, Brown KM, Lynch JP (2005) Root architectural tradeoffs for water and phosphorus acquisition. *Funct Plant Biol* **32**: 737–748
- Hu B, Henry A, Brown KM, Lynch JP (2014) Root cortical aerenchyma inhibits radial nutrient transport in maize (*Zea mays*). *Ann Bot (Lond)* **113**: 181–189
- Jaramillo RE, Nord EA, Chimungu JG, Brown KM, Lynch JP (2013) Root cortical burden influences drought tolerance in maize. *Ann Bot (Lond)* **112**: 429–437
- Julia C, Wissuwa M, Kretschmar T, Jeong K, Rose T (2016) Phosphorus uptake, partitioning and redistribution during grain filling in rice. *Ann Bot (Lond)* **118**: 1151–1162
- Lambers H, Stullen I, van der Werf A (1996) Carbon use in root respiration as affected by elevated atmospheric O<sub>2</sub>. *Plant Soil* **186**: 251–263
- Lascaris D, Deacon J (1991) Relationship between root cortical senescence and growth of wheat as influenced by mineral nutrition, *Idriella bolleyi* (Sprague) von Arx and pruning of leaves. *New Phytol* **118**: 391–396
- Liljeroth E (1995) Comparisons of early root cortical senescence between barley cultivars, *Triticum* species and other cereals. *New Phytol* **130**: 495–501
- Lynch JP (2011) Root phenes for enhanced soil exploration and phosphorus acquisition: tools for future crops. *Plant Physiol* **156**: 1041–1049
- Lynch JP (2013) Steep, cheap and deep: an ideotype to optimize water and N acquisition by maize root systems. *Ann Bot (Lond)* **112**: 347–357
- Lynch JP (2015) Root phenes that reduce the metabolic costs of soil exploration: opportunities for 21st century agriculture. *Plant Cell Environ* **38**: 1775–1784
- Lynch JP, Chimungu JG, Brown KM (2014) Root anatomical phenes associated with water acquisition from drying soil: targets for crop improvement. *J Exp Bot* **65**: 6155–6166
- Lynch JP, Ho MD (2005) Rhizoeconomics: carbon costs of phosphorus acquisition. *Plant Soil* **269**: 45–56
- Lynch JP, Nielsen KL, Davis RD, Jabllokow AG (1997) SimRoot: modelling and visualization of root systems. *Plant Soil* **188**: 139–151
- Lynch JP, Wojciechowski T (2015) Opportunities and challenges in the subsoil: pathways to deeper rooted crops. *J Exp Bot* **66**: 2199–2210
- McElgunn JD, Harrison CM (1969) Formation, elongation, and longevity of barley root hairs. *Agron J* **61**: 79–81
- Miguel MA, Postma JA, Lynch JP (2015) Phene synergism between root hair length and basal root growth angle for phosphorus acquisition. *Plant Physiol* **167**: 1430–1439
- Monteith JL (1965) Evaporation and environment. *Symp Soc Exp Biol* **19**: 205–234
- Pieruschka R, Poorter H (2012) Phenotyping plants: genes, phenes and machines. *Funct Plant Biol* **39**: 813–820
- Postma JA, Dathe A, Lynch JP (2014) The optimal lateral root branching density for maize depends on nitrogen and phosphorus availability. *Plant Physiol* **166**: 590–602
- Postma JA, Kuppe C, Owen MR, Mellor N, Griffiths M, Bennett MJ, Lynch JP, Watt M (2017) OpenSimRoot: widening the scope and application of root architectural models. *New Phytol* **215**: 1274–1286
- Postma JA, Lynch JP (2011a) Theoretical evidence for the functional benefit of root cortical aerenchyma in soils with low phosphorus availability. *Ann Bot (Lond)* **107**: 829–841
- Postma JA, Lynch JP (2011b) Root cortical aerenchyma enhances the growth of maize on soils with suboptimal availability of nitrogen, phosphorus, and potassium. *Plant Physiol* **156**: 1190–1201
- Postma JA, Lynch JP (2012) Complementarity in root architecture for nutrient uptake in ancient maize/bean and maize/bean/squash polycultures. *Ann Bot (Lond)* **110**: 521–534
- R Core Team (2014) R: A Language and Environment for Statistical Computing. R Foundation for Statistical Computing, Vienna, Austria
- Robinson D (1990) Phosphorus availability and cortical senescence in cereal roots. *J Theor Biol* **145**: 257–265
- Rubio G, Walk T, Ge Z, Yan X, Liao H, Lynch JP (2001) Root gravitropism and below-ground competition among neighbouring plants: a modelling approach. *Ann Bot (Lond)* **88**: 929–940
- Saengwilai P, Nord EA, Chimungu JG, Brown KM, Lynch JP (2014) Root cortical aerenchyma enhances nitrogen acquisition from low-nitrogen soils in maize. *Plant Physiol* **166**: 726–735
- Schneider HM, Wojciechowski T, Postma JA, Brown KM, Lücke A, Zeisler V, Schreiber L, Lynch JP (2017) Root cortical senescence decreases root respiration, nutrient content and radial water and nutrient transport in barley. *Plant Cell Environ* **40**: 1392–1408
- Schnyder H (1993) The role of carbohydrate storage and redistribution in the source-sink relations of wheat and barley during grain filling: a review. *New Phytol* **123**: 233–245
- Šimůnek J, Huang K, van Genuchten MT (1995) The SWMS\_3D code for simulating water flow and solute transport in three-dimensional variably saturated media, Version 1.0. Research Report No. 139. U.S. Salinity Laboratory, USDA-ARS, Riverside, CA
- Trachsel S, Kaeppeler SM, Brown KM, Lynch JP (2013) Maize root growth angles become steeper under low N conditions. *Crop Res* **140**: 18–31
- Veneklaas EJ, Lambers H, Bragg J, Finnegan PM, Lovelock CE, Plaxton WC, Price CA, Scheible WR, Shane MW, White PJ, et al (2012) Opportunities for improving phosphorus-use efficiency in crop plants. *New Phytol* **195**: 306–320
- Wissuwa M (2003) How do plants achieve tolerance to phosphorus deficiency? Small causes with big effects. *Plant Physiol* **133**: 1947–1958
- York LM, Nord EA, Lynch JP (2013) Integration of root phenes for soil resource acquisition. *Front Plant Sci* **4**: 355
- York LM, Silberbush M, Lynch JP (2016) Spatiotemporal variation of nitrate uptake kinetics within the maize (*Zea mays* L.) root system is associated with greater nitrate uptake and interactions with architectural phenes. *J Exp Bot* **67**: 3763–3775
- Zhan A, Lynch JP (2015) Reduced frequency of lateral root branching improves N capture from low-N soils in maize. *J Exp Bot* **66**: 2055–2065
- Zhang C, Postma JA, York LM, Lynch JP (2014) Root foraging elicits niche complementarity-dependent yield advantage in the ancient ‘three sisters’ (maize/bean/squash) polyculture. *Ann Bot (Lond)* **114**: 1719–1733
- Zhu J, Brown KM, Lynch JP (2010) Root cortical aerenchyma improves the drought tolerance of maize (*Zea mays* L.). *Plant Cell Environ* **33**: 740–749
- Zhu J, Kaeppeler SM, Lynch JP (2005) Topsoil foraging and phosphorus acquisition efficiency in maize (*Zea mays*). *Funct Plant Biol* **32**: 749–762
- Zhu XG, Lynch JP, LeBauer DS, Millar AJ, Stitt M, Long SP (2016) Plants in silico: why, why now and what? An integrative platform for plant systems biology research. *Plant Cell Environ* **39**: 1049–1057
- Zimmermann HM, Hartmann K, Schreiber L, Steudle E (2000) Chemical composition of apoplastic transport barriers in relation to radial hydraulic conductivity of corn roots (*Zea mays* L.). *Planta* **210**: 302–311